JACS Au
AN OPEN ACCESS JOURNAL OF THE AMERICAN CHEMICAL SOCIETY

pubs.acs.org/jacsau
Article

Carbonyl Migration in Uronates Affords a Potential Prebiotic Pathway for Pentose Production

Ruiqin Yi,* Mike Mojica, Albert C. Fahrenbach, H. James Cleaves, II, Ramanarayanan Krishnamurthy,* and Charles L. Liotta*

Cite This: JACS Au 2023, 3, 2522−2535

Read Online

ACCESS | Metrics & More | Article Recommendations | Supporting Information

ABSTRACT: Carbohydrate biosynthesis is fundamental to modern terrestrial biochemistry, but how this collection of metabolic pathways originated remains an open question. Prebiotic sugar synthesis has focused primarily on the formose reaction and Kiliani−Fischer homologation; however, how they can transition to extant biochemical pathways has not been studied. Herein, a nonenzymatic pathway for pentose production with similar chemical transformations as those of the pentose phosphate pathway is demonstrated. Starting from a C6 aldonate, namely, gluconate, nonselective chemical oxidation yields a mixture of 2-oxo-, 4-oxo-, 5-oxo-, and 6-oxo-uronate regioisomers. Regardless at which carbinol the oxidation takes place, carbonyl migration enables β-decarboxylation to yield pentoses. In comparison, the pentose phosphate pathway selectively oxidizes 6-phosphogluconate to afford the 3-oxo-uronate derivative, which undergoes facile subsequent β-decarboxylation and carbonyl migration to afford ribose 5-phosphate. The similarities between these two pathways and the potential implications for prebiotic chemistry and protometabolism are discussed.

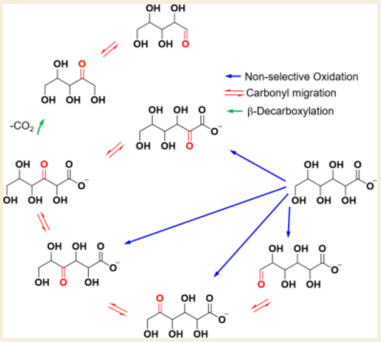

KEYWORDS: *aldonate, β-decarboxylation, Fenton reaction, nonenzymatic oxidation, pentose phosphate pathway, prebiotic sugar synthesis, protometabolism, origins of life, Kiliani−Fischer homologation, glyoxylose reaction*

The transition from abiotic chemistry to life may have taken place gradually, albeit punctuated by leaps in complexity, until eventually arriving at the first viable primitive cellular life forms.[1] How the earliest sugar formation chemistries evolved into the extant sugar synthesis metabolic pathways is still not understood. Some recent studies have looked at catalytic degradation of glucose 6-phosphate under conditions mimicking the Archean ocean, revealing pathways that are comparable to modern glycolysis.[2,3] It is possible that the pathways now principally catalyzed by enzymes were originally templated by ancient abiotic geochemical networks.[4] These abiotic networks may have used some of the same reaction mechanisms observed in cells today.[5] Although enumerating all of the modern biochemical pathways that can occur nonenzymatically is now a tractable problem,[6] it is also likely to be fruitful to experimentally discover novel nonenzymatic reactions and reaction networks, which are constructed using common biochemical transformations that may trace their roots back to the origins of metabolism.[2,3,7−12]

The formose reaction[13,14] is often cited as a prebiotic source of monosaccharides, in particular, ribose and other pentoses.[15,16] An important aspect of the formose reaction is carbonyl migrations that take place through either 1,2-hydride shifts[17] or enediol rearrangements.[18] However, without further stabilization of the pentoses formed, e.g., by prebiotic borate ester synthesis made possible in borate-rich geochemical environments,[19−21] these sugars quickly decompose at the high pH and high-Ca^{2+} concentrations needed for the formose mechanism.[22−24] Note that borate also inhibits the formose reaction, suggesting that the formose reaction and borate ester formation might need to occur in separate locations. The general instability of sugars under prebiotic conditions, sometimes referred to as the "tar problem",[25,26] leads to additional questions about the plausibility of prebiotic nucleoside/tide synthetic pathways[27,28] that require preformed sugars as substrates. While formose-type reactions might have supplied ancient Earth with sugars, how might an early primitive metabolism have afforded a sustainable availability of pentoses?

Larralde et al.[29] suggested that aldonic acids formed as Kiliani−Fischer reaction[30] byproducts could have acted as a more stable repository for carbohydrates in a protometabolic network (Scheme 1, top). This hypothesis is supported by the carbohydrate species found in the Murchison meteorite,[31,32] which contains a high abundance of aldonic acids relative to aldoses. The question then becomes, can aldonic acids be transformed back into carbohydrates like ribose such that they

Received: June 8, 2023
Revised: August 15, 2023
Accepted: August 15, 2023
Published: September 7, 2023

Scheme 1. Reaction Pathway for the Synthesis of Pentoses from C6-Aldonates[a]

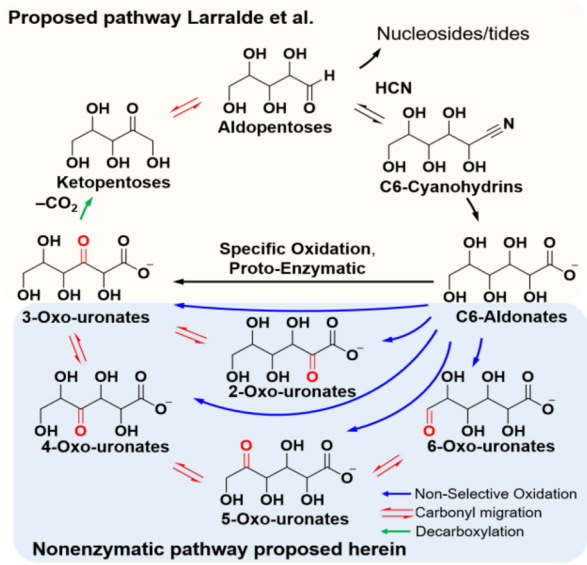

[a]In the top frame is shown the hypothesis proposed by Larralde et al.,[29] in which a primitive enzyme can selectively oxidize C6-aldonates at the 3-position to produce 3-oxo-uronate(s) followed by β-decarboxylation to afford a mixture of pentoses. The nonenzymatic pathway proposed here is shown in the bottom frame and starts with a nonselective chemical oxidation of aldonates, yielding a mixture of 2-oxo-, 4-oxo, 5-oxo-, and 6-oxo-uronate regioisomers. These newly formed uronates can undergo carbonyl migration to the 3-position, following β-decarboxylation to pentoses. The proposed pathway by Larralde et al. in Scheme 1 was reproduced with permission from ref 29. 1995 United States National Academy of Sciences.

can be utilized in prebiotic reactions like nucleoside/tide synthesis?

Larralde et al.[29] also suggested (but did not investigate) that a primitive enzyme could have oxidized C6-aldonates at C3 to yield 3-oxo-uronate derivatives, which could then undergo β-decarboxylation to afford ketopentoses before rearranging to aldopentoses (Scheme 1, top). Before the emergence of primitive enzymes, it is possible that nonselective chemical oxidation of aldonates to uronates could have occurred under prebiotic conditions (e.g., via peroxides or other radiation-produced oxidants[33]). Nonregioselective abiotic oxidation is expected to produce a mixture of uronic acids. Oxidation at the C3 position will enable spontaneous β-decarboxylation, however, oxidation at other positions will produce uronates whose carbonyl group has to migrate to the C3 position to enable β-decarboxylation[34] (Scheme 1, bottom).

Classically, carbonyl migration can occur via rearrangements involving enediol intermediates. Aldoses are converted to ketoses via enediol(ate) intermediates through both general acid and base catalysis. This interconversion of aldoses and ketoses, known as the Lobry de Bruyn–Alberda van Ekenstein transformation, was first identified in 1885 and has been characterized under acid/base[35−38] and calcium[39]/transition-metal-cation[40]-catalyzed conditions (more recent reports have demonstrated that carbonyl migration can occur via 1,2-hydride shifts[17]). Some studies have shown that keto-keto carbonyl migration can occur across the entire backbone[41] but only in the context of the Maillard process involving reactions of glucuronic acid or aldoses with lysine and peptides that form Amadori intermediates,[42−44] ultimately yielding 3-hydroxypyridinium and quinoxaline derivatives. However, whether carbonyl migration can occur in C6-uronates to afford 3-oxo-urnoates for β-decarboxylation in the absence of amino acids and peptides to yield pentoses has not as yet been investigated systematically. The well-documented aldo-to-keto transformation for sugars suggests that the initial migration from the terminal 6-oxo to 5-oxo position in C6-uronates should be possible, but keto-to-keto migrations in sugars as well as C6-uronates (e.g., 5-oxo to 4-oxo to 3-oxo) are not well studied.

Herein, a prebiotically plausible, nonregioselective oxidation of a C6-aldonate affording a mixture of C6-uronate regioisomers is demonstrated using ferrous iron and hydrogen peroxide. These C6 2-oxo-, 4-oxo-, 5-oxo-, and 6-oxo-uronate isomers can undergo carbonyl migration to generate 3-oxo-uronates, which then undergo β-decarboxylation yielding all four aldopentoses, namely, ribose, arabinose, xylose, and lyxose.

The implications of this chemistry that converts aldonates to uronates to pentoses (Scheme 2a) are further discussed in the

Scheme 2. Similarities between Proposed Protometabolic and Biotic Pentose Phosphate Pathways[a]

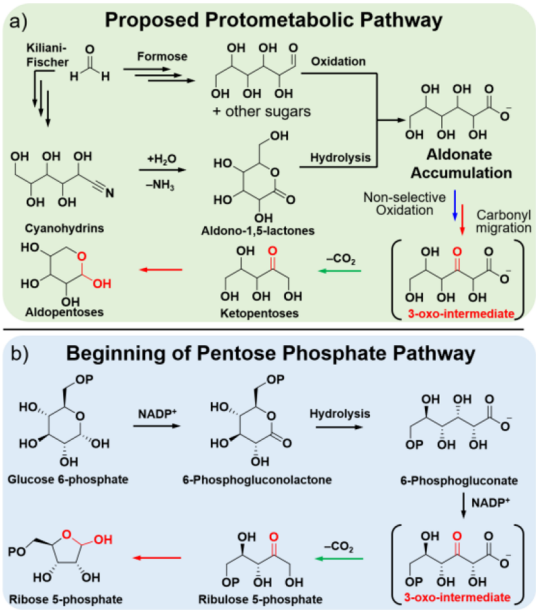

[a](a) Proposed protometabolic pentose pathway leading to the accumulation of aldonates followed by nonselective oxidation to uronates, carbonyl migration, and β-decarboxylation. (b) First few steps of the pentose phosphate pathway shown for comparison (the abbreviation OP in the chemical structures indicates phosphate).

context of possible carbohydrate protometabolic networks that utilized similar chemical transformations as those found in extant enzyme-directed biochemical carbohydrate metabolism, in particular, the first steps of the extant pentose phosphate pathway (PPP, Scheme 2b), which converts glucose 6-phosphate to ribose 5-phosphate. It is proposed that the more stable aldonates, as opposed to the less stable aldoses and ketoses, could have accumulated on prebiotic Earth being generated through Kiliani–Fischer homologation.[45] In a manner analogous to the PPP, these aldonates could have then been oxidized albeit nonselectively to uronates, which

https://doi.org/10.1021/jacsau.3c00299
JACS Au 2023, 3, 2522−2535

after carbonyl migration to the β-positions would yield ketose and aldose sugars following decarboxylation.

RESULTS

Oxidation of Gluconate by Fenton's Reagent

The Fenton reaction employing ferrous iron and H_2O_2 is attractive from a prebiotic perspective because ferrous iron[46,47] and H_2O_2[48] may have been geochemically available on early Earth. Fenton's reagent has been reported by Larsen and Smidsrød[49] to afford the oxidation of aldonic acids to uronic acids; however, the available analytical tools employed at the time of this study limited product identification. Therefore, an experiment to demonstrate the nonselective oxidation of an aldonate to uronate regioisomers using Fenton's reagent[33] was carried out. An aqueous solution containing 500 mM sodium gluconate **1** and 25 mM ferrous acetate was prepared, and the pH was adjusted to 3. Then, the mixture was placed on an ice bath while 1 equiv of H_2O_2 was added slowly (Figure 1a). The reaction was then warmed back to room temperature. After ~2 h, the iron cations were removed from the mixture, and the ^{13}C NMR spectrum was recorded. The NMR spectrum revealed a number of new resonances that indicate the oxidation of **1** to four uronate regioisomers, namely, **2**p, **3**f, **4**, and **5**p/**5**f (p denotes the pyranose form and f the furanose form). Although 1 equiv of H_2O_2 was used, the reaction mixture still contained a significant amount of the starting material. New resonances were assigned by comparison with signals of authentic uronate standards under identical conditions. Figure 1b shows partial ^{13}C NMR spectra focusing on the anomeric carbon, carboxylate, and ketone regions for both the reaction mixture and standards (for the full ^{13}C NMR spectra and complete resonance assignments, see Figure S1). The region between 93 and 105 ppm reveals pyranose/furanose anomeric carbon signals, which are assigned to α,β-pyranose-guluronate **2**p (94.3 and 93.6 ppm), β-furanose-5-keto-gluconate **3**f (103.8 ppm), α-pyranose **5**p (98.0 ppm), and β-furanose-2-keto-gluconate **5**f (100.4 ppm). Meanwhile, a signal around 212 ppm, which is assigned to the ketone carbon of *xylo*-4-hexulosonate **4**, was also observed. Note that a similar product distribution was observed when the reaction was heated at 50 °C for 2 h (Figure S3).

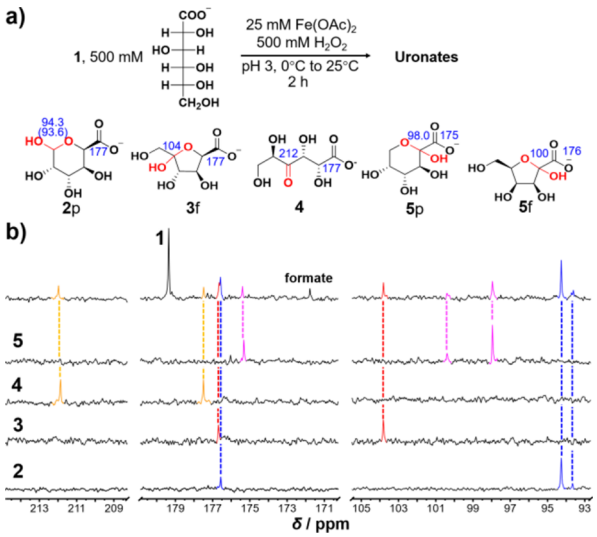

Figure 1. Oxidation of gluconate by Fenton's reagent. (a) Scheme for the oxidation of gluconate **1** to uronates **2**−**5** by the Fenton reaction. The chemical shifts for anomeric and carbonyl carbon resonances are shown in blue next to the respective carbons of each uronate (the chemical shift for the β-anomer of **2**p is shown in parentheses). (b) Partial ^{13}C NMR spectra recorded in 10% D_2O after oxidation and removing iron using cation exchange resin by the following procedure. DOWEX 50Wx4 100−200 mesh (~500 mg) (H) cation exchange resin was added to the reaction mixture, vortexed for 2 min, and filtered. Phosphate buffer was added to the filtrate in order to adjust the pH to 7.5. Note that without pH adjustment, 2-oxo aldonic acids tend to cyclize to form ascorbic acid and its isomers under acidic conditions.[91] The results indicate that uronates α,β-pyranose-guluronate **2**p (blue), β-furanose-5-keto-gluconate **3**f (red), xylo-4-hexulosonate **4** (orange), and α-pyranose- and β-furanose-2-keto-gluconate **5**p/**5**f (pink) from the oxidation of **1** were synthesized. The resonances were assigned by comparing with the signals of standards **2**−**5** under identical conditions. Note that a similar product distribution was observed when the H^+ form resin was used instead of the Na^+ form (Figure S2), suggesting that the resin itself does not significantly affect the products obtained after oxidation.

Oxidation of gluconate **1** was complete after no more than 2 h, since no significant difference in the product distribution was observed even when the reaction time was prolonged to 32 h (Figure S4). This result also suggests that further oxidation of the uronate products is negligible, at least when using 1 equiv of H_2O_2. Moreover, gluconate oxidation did not occur when Fe(II) or H_2O_2 was omitted (Figure S5). Higher initial concentrations of Fe(II) still did not yield any detectable uronates or pentoses even when the reaction was carried out at a higher temperature (70 °C) in the absence of H_2O_2 (Figure S6). These results are consistent with previous reports that oxidation by the Fenton reaction occurs[50] through the hydroxyl radical (•OH), which is catalytically generated by the reaction of H_2O_2 with Fe(II).

The same Fenton oxidation was also tested at initial pH values of 2, 3, 4, 5, 7, and 9 (Figure S7). Reactions at pH 2, 3, and 4 yielded similar amounts of uronic acids **2**p, **4**, **3**f, and **5**f along with a trace amount of arabinose, a product which is hypothesized to come about by Ruff degradation[51] of the gluconate starting material. At pH 5 and 7, relatively minor amounts of uronic acids were observed, while Ruff degradation to arabinose increased in yield. When the reaction was carried out at pH 9, both Ruff degradation and oxidation yields became very low. The yields of uronates and arabinose were quantified using $^{13}C_6$-labeled gluconate and HPLC (see Figures S8, S59 and Tables 1, S1). These results are consistent with previous reports[49] that the selectivity of oxidation and Ruff degradation are pH-dependent; pH < 5 favors non-

Table 1. Total Yields of Uronates Recorded from ^{13}C NMR Spectra (Figure S8) and the Yield of Arabinose Quantified by HPLC Analysis (Figure S59) Starting from Gluconate 1 under the pH Noted

pH	uronates/%[a]	arabinose/%	remaining S.M./%
2	51	1	44
3	50	2	42
4	47	7	42
5	15	24	39
7	8	26	48

[a]The yields of uronates were calculated using the integrated ratio of uronate carboxylate resonances and the gluconate carboxylate resonance in each spectrum of Figure S8.

https://doi.org/10.1021/jacsau.3c00299
JACS Au 2023, 3, 2522−2535

selective oxidation and pH 5 to 7 favors Ruff degradation. Completely selective Ruff degradation was not able to be achieved under the conditions tested. Phosphate (0.5 M) was also included in the Fenton reaction (pH 3, 5, or 7), and Ruff degradation was almost completely inhibited across the three pH values, while uronate production still occurred but became significantly inhibited at pH 7 (Figure S9). These results indicate that this type of Fenton oxidation step has a limited pH[49] and temperature range[52] and may constrain where such transformations can take place on early Earth.

As shown in Scheme S1, the generation of uronate regioisomers **2** to **5** oxidized at the C6, C5, C4, and C2 positions of gluconate **1**, respectively, is an indication of the nonselective nature of this reaction, with one exception. The uronate regioisomer produced by oxidation at the C3 (beta) position of **1** was not observed. Note that some of the arabinose immediately observed after Fenton oxidation may also be the result of oxidation at the 3-position, which yields selectively after rapid β-decarboxylation the arabinose stereoisomer as a result of chelation by iron to the enediolate intermediate that would only expose one face of the double bond. However, arabinose was also observed after aqueous gamma radiolysis (which generates a combination of •OH, •H, and hydrated electrons) of **1** in the absence of any iron (Figure S54), an observation which supports the radical-based Ruff degradation mechanism. Moreover, to the best of our knowledge, there is no reported synthetic procedure for this 3-oxouronate and has only been observed enzymatically in studies of the pentose phosphate pathway,[53,54] but was not fully characterized in those reports. We also were unable to find the reports for the synthesis of other C6 3-oxo-uronates via this procedure (Fe^{2+}/H_2O_2) in the literature.

Carbonyl Migration in C6-Uronates Affords β-Decarboxylation Yielding Pentoses

Having confirmed the presence of 2-oxo, 4-oxo, 5-oxo, and 6-oxo uronates by the oxidation of the aldonate **1**, the next key question becomes whether the carbonyl group of these uronates has the potential to migrate to the C3-position in order to allow β-decarboxylation to pentoses. A study by Hall et al.[55] demonstrated that 2-keto-gluconate under alkaline conditions in the presence of Ca^{2+} at 100 °C yields ribulose and arabinose, which the authors also suggest occurs via carbonyl migration to a 3-oxo-uronate followed by β-decarboxylation. To test this supposition, we conducted a series of experiments under weakly basic or neutral conditions employing uronates with carbonyls at the C2, C4, C5, and C6 positions, namely, compounds **5**, **4**, **3**, and **15**, respectively. Note that 2-oxo and 4-oxo uronates only require one carbonyl migration to generate the 3-oxo uronate needed for β-decarboxylation, while 5-oxo and 6-oxo uronates require two and three carbonyl migrations toward the carboxylate terminus, respectively.

From 2-Oxo-uronate 5

A solution of 2-keto-gluconate **5** was prepared (500 mM in 10% D_2O) at pH 8 with 0.9 M sodium phosphate buffer (Figure 2a). We chose phosphate buffer since it allowed for transparent detection using ^{13}C NMR spectroscopy of bicarbonate formed by CO_2 evolution from β-decarboxylation. (Bi)carbonate buffer, although better at buffering alkaline pH, would have interfered with assessing the bicarbonate formed from β-decarboxylation. Phosphate as a buffer also has biochemical relevance and potential prebiotic plausibility;[56,57]

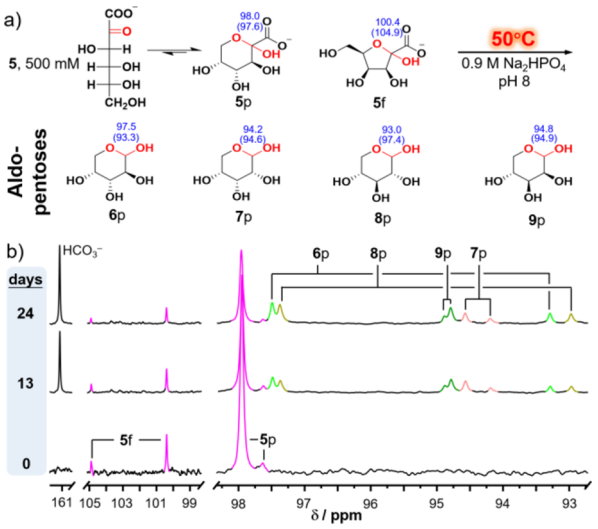

Figure 2. From 2-keto-gluconate to pentoses. (a) Scheme for the reaction of 2-keto-gluconate **5** to pentoses **6**–**9**. The chemical shifts for the anomeric carbon resonances are shown in blue next to the respective carbons for each uronate (chemical shifts for the β-anomers are shown in parentheses). (b) Partial ^{13}C NMR spectra of the anomeric carbon region recorded on the reaction of 2-keto-gluconate at an initial pH of 8 in 10% D_2O buffer before heating (t = 0 day) and after heating at 50 °C for 13 and 24 days. Note that the reaction of 2-keto-gluconate at pH 9 and 25 °C was also performed (Figures S14 and S15).

however, such large concentrations of phosphate may be globally unlikely but were employed here to maintain the pH. Note that phosphate anion can serve as a general-base catalyst[41,58] for carbonyl migration in sugars at neutral pH. The reaction mixture was monitored at 50 °C by ^{13}C NMR spectroscopy (see SI, Figures S11–S13). The initial spectrum (t = 0) revealed four major signals[59] belonging to the α/β-anomers of the furanose- and pyranose-isomers **5**f and **5**p in the region between 97 and 105 ppm (Figure 2b). The ratio of signal intensities for α/β-**5**p to α/β-**5**f is approximately 39:11, suggesting that ∼78% of **5** exists in the pyranose form in the solution. The linear form of **5** was not detected.

This solution of **5** was heated at 50 °C over the course of a few weeks. After 2 days, a new signal at 162 ppm assigned to bicarbonate was observed (see SI, Figure S13). This bicarbonate signal increased in intensity over time, and the pH of the reaction decreased to approximately 7.4 after 7 days. After 13 days, a set of signals arising from aldopentoses was observed. Figure 2b shows the anomeric region of the ^{13}C NMR spectrum and displays these resonances assigned to α,β-arabinopyranose **6**p (α-anomer 97.5 ppm, β-anomer, 93.3 ppm), α,β-ribopyranose **7**p (β-anomer, 94.6 ppm, α-anomer 94.2 ppm), α,β-xylopyranose **8**p (β-anomer, 97.4 ppm, α-anomer 93.0 ppm), and α,β-lyxopyranose **9**p (β-anomer, 94.9 ppm, α-anomer 94.8 ppm).[60] Trace amounts of the pentuloses, ribulose **10**, and xylulose **11** were also detected in the ^{13}C NMR data, and their presence was confirmed by HPLC analysis (see SI, Figures S12 and S60a).

The observation of these pentoses along with bicarbonate can be explained by invoking carbonyl migration followed by β-decarboxylation, a pathway that has been shown to occur in the "glyoxylate scenario".[61] The proposed reaction pathway is shown in Scheme 3. Carbonyl migration from C2 to C3 (3-oxo) allows β-decarboxylation to take place at a relatively rapid

https://doi.org/10.1021/jacsau.3c00299
JACS Au 2023, 3, 2522–2535

Scheme 3. Proposed Reaction Pathway of 2-Oxo-uronate 5 to Aldopentoses Generated via Carbonyl Migration, Epimerization, and β-Decarboxylation (the Linear Forms Are Depicted To Show the Carbonyl Migration)

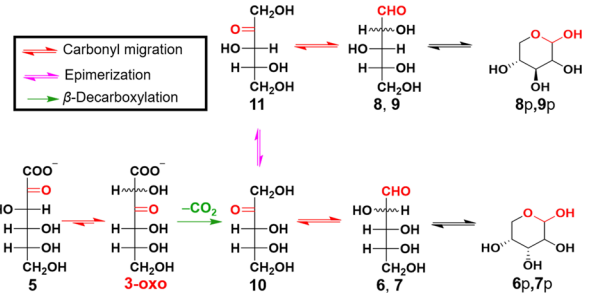

rate such that no obvious signals in the ^{13}C NMR spectrum which could be assigned to this 3-oxo regioisomer were observed. β-Decarboxylation yields ribulose **10**, which undergoes reversible carbonyl migration to form arabinose **6** and ribose **7**. Ribulose **10** can also epimerize to xylulose **11**, which undergoes reversible carbonyl migration to xylose **8** and lyxose **9**. The four pentoses cyclize to their pyranose forms **6**p−**9**p, which are all observed by ^{13}C NMR. Note that **5** preferentially exists as the cyclic hemiacetals **5**p and **5**f; however, carbonyl migration can only take place among the linear forms of these species. The aldonic acid conjugate base, arabinoate, was also observed in the NMR spectrum (see SI, Figure S12), and it is hypothesized that this aldonate is slowly formed by oxidative decarboxylation of **5**, an α-keto acid, produced in the presence of O_2.[62−64] No C5 aldonates like arabinoate were observed in the other 4-oxo-, 5-oxo-, and 6-oxo-uronates studied herein.

After a period of 24 days, a total ∼30.6% yield of pentoses (according to HPLC analysis) was determined: ∼8.5% arabinose **6**, ∼5.7% ribose **7**, ∼8.9% xylose **8**, ∼6.1% lyxose **9**, ∼0.8% ribulose **10**, and ∼0.6% xylulose **11** (Figure S60a). Note that according to the proposed pathway in Scheme 3, arabinose **6** and ribose **7** should be the most abundant with xylose **8** and lyxose **9** the least, however, this is not what is observed. A previous study[58] on pentose isomerization in aqueous solution at 78 °C and pH 7.5 in 0.5 M P_i buffer revealed that xylose and arabinose are more thermodynamically favored than lyxose and ribose at equilibrium. We hypothesize that the relative ratios of pentoses observed are largely a consequence of their relative thermodynamic stability. This hypothesis was further confirmed by preparing an equimolar solution of all four pentoses and allowing it to react under similar conditions for 16 days (Figures S16−S18), after which time a similar distribution of arabinose, ribose, xylose, and lyxose was obtained (Figures S18 and S61).

This same reaction starting with urontate **5** was also conducted at room temperature and pH 9 and monitored over a period of 56 days (see SI, Figures S14 and S15). The 2-ketogluconate (∼20%) was consumed (see the SI, Figure S37a) and the total yield of C5 sugars obtained was lower (∼10.5%): ∼2.8% arabinose **6**, ∼2.8% ribose **7**, ∼1.3% xylose **8**, ∼2.6% lyxose **9**, ∼0.4% ribulose **10**, and ∼ 0.6% xylulose **11** (Figure S60b). These results indicate that raising the reaction temperature increases the rate of carbonyl migration and pentose production. Note that only trace amounts of other uronates besides **5** were detected at either 25 °C or 50 °C, a result which suggests that the 3-oxo-uronates, once formed, rapidly undergo decarboxylation, preventing further carbonyl migration down the uronate chain.

From 4-Oxo-uronate 4

The 4-oxo-uronate D-*xylo*-4-hexulosonate **4** was subjected to similar reaction conditions as **5** but at room temperature and slightly higher pH (0.9 M P_i at pH 9 and 25 °C, see Figure 3a)

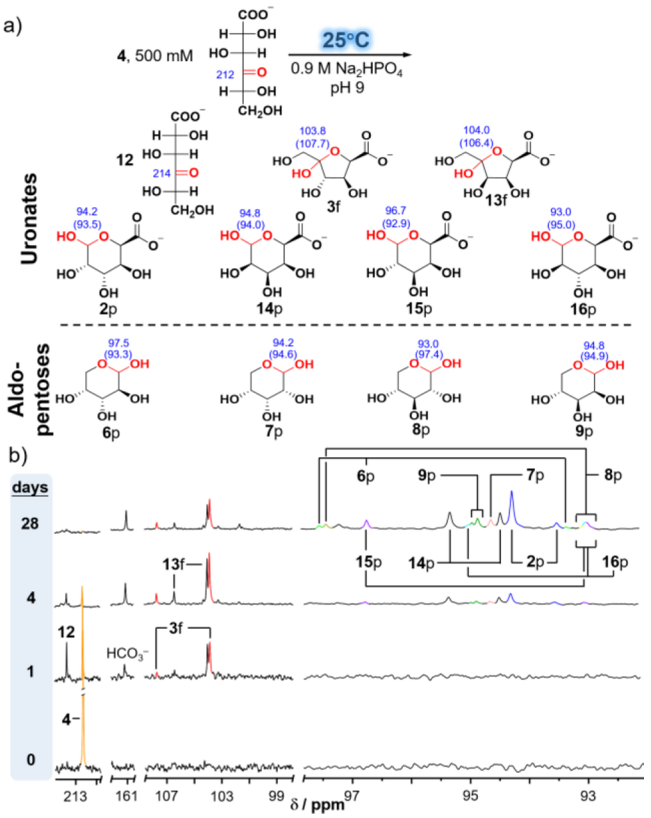

Figure 3. From D-*xylo*-4-hexulosonate to pentoses. (a) Scheme for the reaction of D-*xylo*-4-hexulosonate **4** at an initial pH of 9 in 10% D_2O to afford uronates **2**, **3**, **12**−**16** and aldopentoses **6**−**9**. The chemical shifts for the anomeric and ketone carbon resonances are shown in blue next to the respective carbons for each uronate and pentose (chemical shifts for the β-anomers are shown in parentheses). For more details of the spectral assignments, see Figures S20−S22. (b) Partial ^{13}C NMR spectra highlighting the anomeric carbon and ketone regions recorded on the reaction of D-*xylo*-4-hexulosonate **4** from 0 to 28 days.

and monitored by ^{13}C NMR spectroscopy (see SI, Figures S19−S23). The initial spectrum (Figure 3b) reveals a signal at 212 ppm, the resonance of which arises from the ketone carbon, and indicates **4** exists in its linear form. The fact that the carbonyl is on C4 prevents the formation of pyranose or furanose cyclic hemiacetals. After 1 day, a new resonance in this same region at 214 ppm was observed, a signal that is consistent with the C5 epimer, namely, L-*arabino*-4-hexulosonate **12**. In addition to **12**, four new resonances, in the region of 103−108 ppm, assigned to the anomeric carbons of two 5-oxo-uronates were observed: α,β-furanose-5-keto-D-gluconate **3**f (α-anomer 107.7 ppm, β-anomer, 103.8 ppm),[65] which was confirmed by comparison to an authentic standard and its epimeric α,β-furanose-L-tagaturonate **13**f (106.4 and 104.0 ppm). Also, after 1 day, a signal belonging to bicarbonate observed at 161 ppm appeared in the spectrum and continued to increase over time (see Figure S23). The pH of the solution

https://doi.org/10.1021/jacsau.3c00299
JACS Au 2023, 3, 2522−2535

fell to 7.6 after 4 days. After 28 days, the signals for both **12** and **4** were no longer detected, while a set of new signals appeared in the anomeric carbon region from 92 to 98 ppm and were assigned to the mixture of pentoses (**6**p−**9**p) and 6-oxo-uronates (**2**p, **14**p−**16**p).

Carbonyl migration from the C5-oxo-epimers **13** and **3** to the C6-oxo-epimers results in a mixture of stereoisomers (Figures S21 and S22), namely, *α*,*β*-pyranose-guluronate **2**p (94.2 and 93.5 ppm), *α*,*β*-pyranose-taluronate **14**p (94.8 and 94.0 ppm), *α*,*β*-pyranose-galacturonate **15**p (*β*-anomer 96.7 ppm and *α*-anomer 92.9 ppm),[66] and *α*,*β*-pyranose-iduronate **16**p (*α*-anomer 95.0 ppm and *β*-anomer 93.0 ppm).[67] Resonances for all four aldopentoses **6**p−**9**p were also identified in addition to[68] ribulose **10** and xylulose **11** (Figures S21 and S22). After 28 days, ∼70% of 5-oxo and 6-oxo-uronates remained (see SI, Figure S37b) and the total yield of C5 pentoses was determined by HPLC to be ∼10.2%: ∼2.2% arabinose **6**, ∼1.5% ribose **7**, ∼2.1% xylose **8**, ∼3.3% lyxose **9**, ∼0.4% ribulose **10**, and ∼ 0.7% xylulose **11** (Figure S62).

All the products identified from ^{13}C NMR spectroscopy (Figure 3b) and the order of appearance of each uronate regioisomer provide a basis for understanding how carbonyl migration takes place along the carbon chain of **4**. The proposed pathway is displayed in Scheme 4. First, carbonyl

Scheme 4. Proposed Reaction Pathway for Carbonyl Migration of 4 That Generates the 5-Oxo-Uronates and 6-Oxo-Uronates Observed in Addition to the 3-Oxo-Uronates, Which Lead to Pentose Formation (the Linear Forms Are Depicted To Show the Carbonyl Migrations)

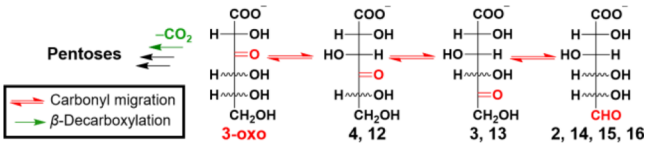

migration from C4 to C3 explains the formation of pentoses via the same mechanistic transformations involving *β*-decarboxylation as proposed for 2-keto-gluconate **5**, as shown in Scheme 4. The sequence of appearance of 5-oxo-uronate epimers **3** and **13** before 6-oxo-uronate stereoisomers **2**, **14**, **15** and **16** is also best explained by carbonyl migration. The fact that **4** relatively quickly epimerizes to **12** at approximately the same rate as the appearance of 5-oxo-uronates **3** and **13** is also consistent with the proposed mechanism since it is expected that production of these compounds all proceed through the same enediol(ate) intermediate. Note that ∼99.0% pure phosphate buffer was used, which contained max 0.02% calcium, and this metal impurity could potentially influence the mechanism, if acting catalytically. The 5-oxo-uronates preferentially adopt the furanose ring forms **3**f and **13**f, while the 6-oxo-uronates are observed predominantly as their pyranose-cyclic hemiacetals **2**p, **14**p, **15**p, and **16**p. In comparison to the results for 2-keto-gluconate **5**, the increase in concentration of bicarbonate occurred more rapidly in the reaction of **4** under identical conditions. After 28 days, **4** was completely consumed, while much of **5** still remained (see SI, Figure S37a). These observations suggest that carbonyl migration is more facile in the case of **4** than **5**, a feature which can be explained by the mechanism of carbonyl migration, which requires the linear aldehyde or ketose to form before an enediol(ate) tautomer can result. The 4-oxo-uronate **4** is predominantly in the linear ketose form, being structurally incapable of forming furanose- or pyranose-cyclic hemiacetals, while the 2-oxo-uronate **5** is detected only as its furanose- and pyranose-cyclic hemiacetals *α*,*β*-**5**p and *α*,*β*-**5**f.

From 5-Oxo-uronate 3

The same reaction starting with 5-oxo-urontate **3** was also conducted at room temperature and pH 9 (see Figures S24−S26). The initial spectrum shown in Figure 4 displays two

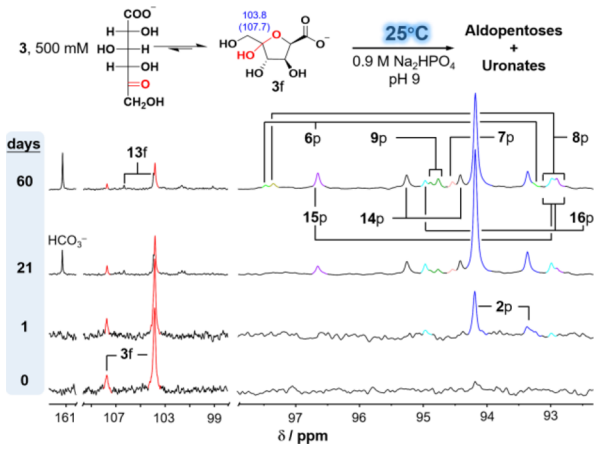

Figure 4. From 5-keto-gluconate to pentoses. Partial ^{13}C NMR data of the anomeric carbon region recorded on the reaction of 5-keto-gluconate **3** at an initial pH of 9 in 10% D_2O over a period of 60 days yielding uronates **2**, **13**−**16**, and pentoses **6**−**9**.

major resonances in the anomeric region, which are assigned to *α*,*β*-furanose-5-keto-gluconate **3**f. After 1 day, two new signals were observed and assigned to the 6-oxo-uronate, *α*,*β*-pyranose-guluronate **2**p. After 5 days (see Figure S26), new signals for the epimers of **3** and **2**, namely, **13** and **16**, respectively, were detected as their cyclic hemiacetals. The above experiments indicate that the initial carbonyl migration of 5-oxo-uronate **3** results in 6-oxo-uronate **2** observed as its pyranose form **2**p. The fact that **2**p forms before bicarbonate suggests that the one carbonyl migration from C5 to C6 happens faster than the two migrations from C5 to C3. Moreover, **2**p, a stable 6-membered ring formed in large amount as the major product even after 60 days, seems to serve as a thermodynamic sink, which slows carbonyl migration back toward C3. In comparison to carbonyl migration in **4**, carbonyl migration in **3** is much slower, and the reaction does not consume all of **3** even after 60 days. This fact can be explained by (i) **3** existing predominantly as **3**f (as opposed to the linear form) and (ii) the rapid migration to **2**p, both structures retarding the rate of further carbonyl migration. Nevertheless, even though only trace amounts of **4** and **12** were detected in the ^{13}C NMR spectrum (Figure S25), the accumulation of bicarbonate and pentoses **6**−**9** reveals that carbonyl migration to 3-oxo-uronates followed by *β*-decarboxylation still occurs.

From 6-Oxo-uronate 15

When the 6-oxo-uronate galacturonate **15** solution was monitored at pH 9 over time at 25 °C by ^{13}C NMR spectroscopy (Figure 5), even after standing at 25 °C for 6 months, very little of the galacturonate **15**p had been consumed and no pentoses were observed. HPLC analysis of the reaction mixture (Figure S66) allowed the detection of a

https://doi.org/10.1021/jacsau.3c00299
JACS Au 2023, 3, 2522−2535

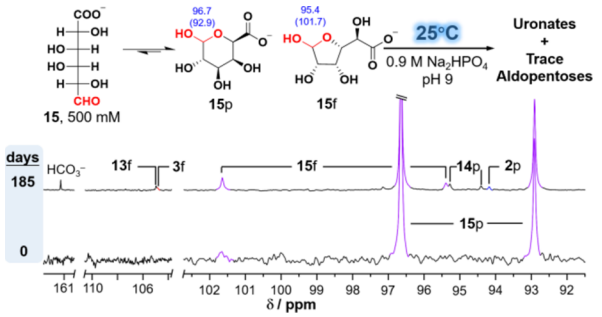

Figure 5. Carbonyl migration of **15**. Partial ^{13}C NMR spectra for carbonyl migration of galacturonate **15** under the conditions shown in the scheme above to afford uronates **2**, **3**, **13**, and **14** after 185 days. The chemical shifts for the anomeric carbon resonances are shown in blue next to the respective carbons for each uronate. Chemical shifts for the β-anomers are shown in parentheses.

small amount of C5 sugars, with a total yield of ∼1.4%: ∼0.3% arabinose **6**, ∼0.3% ribose **7**, 0.2% xylose **8**, 0.4% lyxose **9**, ∼0.1% ribulose **10**, and ∼ 0.1% xylulose **11**. A similar result was obtained, i.e., the apparent rate of carbonyl migration was observed to be equally slow in another 6-oxo-uronate stereoisomer, namely, glucuronate **17**[66] (Figures S45 and S46). As expected, pentose production is even slower than that observed for the 5-oxo-uronate **3**. The slow rate of production can be explained by the stability of the pyranose-cyclic hemiacetal structure of **15** in addition to requiring the most number of carbonyl migrations needed to acheive the 3-oxo-uronate. When the reaction of **15** (described herein) or **17** was repeated at 50 °C (**15**: Figures S38 and S39; **17**: Figures S47–S49), the rate of pentose production significantly increased in comparison to 25 °C. HPLC analysis of the reaction mixture in **15** revealed a total pentose yield of ∼16.5% after 20 days: ∼5.1% arabinose **6**, ∼1.9% ribose **7**, ∼4.9% xylose **8**, ∼3.3% lyxose **9**, ∼0.7% ribulose **10**, and ∼ 0.6% xylulose **11** (Figure 6). HPLC data of the reaction of **17** revealed a similar trend; see Table 2 for more details.

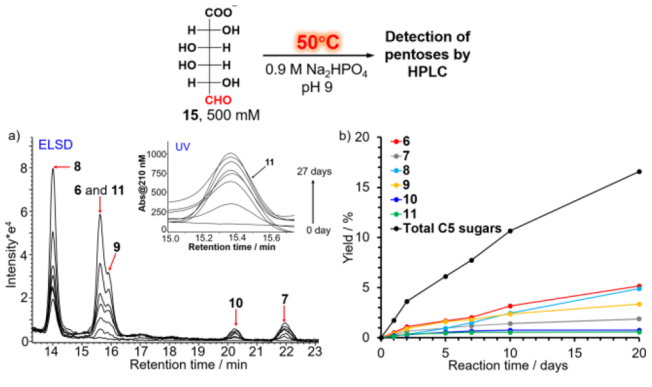

Figure 6. HPLC analysis of pentose formation in the reaction of **15**. (a) Partial HPLC chromatograms with evaporative light-scattering detection (ELSD) and UV absorption (inset) monitoring the reaction of the 6-oxo-uronate **15** at an initial pH of 9 at 50 °C showing the increase in the intensity of the peaks assigned to the pentoses **6**–**11**. Note that the retention time of pentoses **6**–**11** was confirmed by spiking the corresponding standards. (b) Yields of pentoses **6**–**11** as determined by HPLC data shown in (a).

DISCUSSION

Overview of the C6-Uronate Carbonyl Migration and β-Decarboxylation Network

The proposed pathways for the conversion of all uronates to pentoses investigated herein are shown in Scheme 5. Starting from the 2-oxo-uronate **5**, one carbonyl migration leads to the 3-oxo intermediate shown in Scheme 5, which quickly and irreversibly undergoes β-decarboxylation, to afford ribulose **10**. β-Decarboxylation could directly yield arabinose **6** and ribose **7**; however, the more substituted ketose carbonyl is expected[69] to be the favored tautomer immediately formed. Irreversible β-decarboxylation prohibits further carbonyl migration to form 4-oxo-, 5-oxo-, and 6-oxo-uronates. Ribulose **10** can undergo carbonyl migration to arabinose **6** and ribose **7** or epimerize to xylulose **11**, which itself can undergo carbonyl migration to xylose **8** and lyxose **9**. The greater stability of the pyranose-aldopentoses in comparison to the furanose-ketopentoses helps push the equilibrium toward the former.[70] Carbonyl migration might continue down the pentose chain, however, no signals for 3-oxo-pentoses were detected in the ^{13}C NMR spectra. Note that the thermodynamic study of the aqueous equilibria between ribose, ribulose, and arabinose in phosphate buffer[71] suggests that ketopentoses are favored to isomerize into aldopentoses.

The 4-oxo-uronate **4** epimerizes to **12**, which is an L-uronate; hence, carbonyl migration from **4** yields D-3-oxo-uronate stereoisomers, while carbonyl migration from **12** yields the L-stereoisomers. Thus, β-decarboxylation produces a mixture of D- and L-pentoses when starting from **4**. Carbonyl migration from 5-oxo-uronates **3** and **13** also unavoidably yields a mixture of D and L 4-oxo-uronates **4** and **12**, while the 6-oxo-uronates **2**, **14**, **15**, and **16**, which must proceed through either the 5-oxo-uronates **3** or **13**, also undergo the same fate of yielding a mixture of D and L pentose stereoisomers after β-decarboxylation. Indeed, the general expectation is that mixtures of D- and L-pentoses will result from all 4-oxo-, 5-oxo-, and 6-oxo-uronates regardless of the initial stereochemical configurations at each of their asymmetric centers. While it is still possible that D-2-oxo-uronates like **5** may yield D-pentoses selectively, L-pentoses cannot be avoided even when starting from D-enantiomers of 4-oxo-, 5-oxo-, or 6-oxo-uronates, and vice versa, without stereochemical control over the carbonyl migration reaction.

Mass spectrometry experiments carried out in D_2O on the C6-oxo-uronate **17** support the proposed mechanism that carbonyl migration occurs predominantly through enediol(ate) intermediates (Figure S70). In D_2O, enediol(ate) tautomerization to hydroxyaldehydes/ketones will result in the incorporation of deuterium on the carbon chain, which can be measured by mass spectrometry. The results show increasing substitution of deuterium for hydrogen as the reaction progresses. Detailed analysis of the mass spectral data recorded over time suggests that carbonyl migration through 1,2-hydride shifts,[17] a mechanism which would not lead to deuterium incorporation, may contribute to some extent in the carbonyl migration process, but is not the major route. For more details, see the discussion in Scheme S2 in the Supporting Information.

The proposed mechanism can account for the general trends observed for pentose production from the 6-oxo-, 5-oxo-, 4-oxo-, and 2-oxo-uronates investigated. The rates of pentose production (see Table 2) are slowest for 6-oxo-uronates, which

https://doi.org/10.1021/jacsau.3c00299
JACS Au 2023, 3, 2522−2535

Table 2. Time of Appearance of HCO_3^- Recorded from the ^{13}C NMR Spectra and Total Yields[a] of Pentoses Quantified by HPLC Analysis, Starting from Different Uronates under the pH and Temperature Conditions Noted

uronate	conditions	HCO_3^-/days	total C5/%	ribose 6/%	arabinose 7/%	lyxose 8/%	xylose 9/%	ribulose 10/%	xylulose 11/%
2-oxo 5	pH 9, 25 °C, 56 days	4	10.5	2.8	2.8	1.3	2.6	0.4	0.6
	pH 8, 50 °C, 24 days	2	30.6	8.5	5.7	8.9	6.1	0.8	0.6
4-oxo 4	pH 9, 25 °C, 28 days	1	10.2	2.2	1.5	2.1	3.3	0.4	0.7
5-oxo 3	pH 9, 25 °C, 60 days	5	10.6	2.1	2.0	2.2	2.9	0.5	0.9
	pH 8, 25 °C, 96 days	11	8.4	1.9	1.1	1.5	1.8	0.6	1.5
	pH 7, 25 °C, 96 days	18	8.4	2.0	1.0	1.3	1.5	0.8	1.8
	pH 9, 50 °C, 20 days	1	13.5	3.4	1.3	5.6	1.9	0.8	0.5
	pH 8, 50 °C, 20 days	1	17.5	5.3	1.5	7.2	2.2	0.8	0.5
	pH 7, 50 °C, 20 days	2	19.3	5.7	1.8	6.8	3.8	0.5	0.7
6-oxo 15	pH 9, 25 °C, 185 days	10	1.4	0.3	0.3	0.2	0.4	0.1	0.1
	pH 9, 50 °C, 20 days	2	16.5	5.1	1.9	4.9	3.3	0.7	0.6
	pH 8, 50 °C, 15 days	3	14.5	4.3	1.2	4.5	3.2	0.6	0.7
6-oxo 17	pH 9, 25 °C, 78 days	22	0.5	0.1	0.1	0.08	0.09	0.04	0.05
	pH 9, 50 °C, 20 days	2	18.0	6.1	1.5	6.0	2.7	0.8	0.9

[a]These data were measured from HPLC analysis as shown in Figures 6, S60, S62−S64, and S66−S69.

Scheme 5. Proposed Reaction Pathways Showing the Major Routes for Synthesizing Aldopentoses 6p−9p, Achieved from Carbonyl Migration, Epimerization, and β-Decarboxylation of All the 2-Oxo-, 4-Oxo-, 5-Oxo-, and 6-Oxo-uronate Isomers Studied Herein[a]

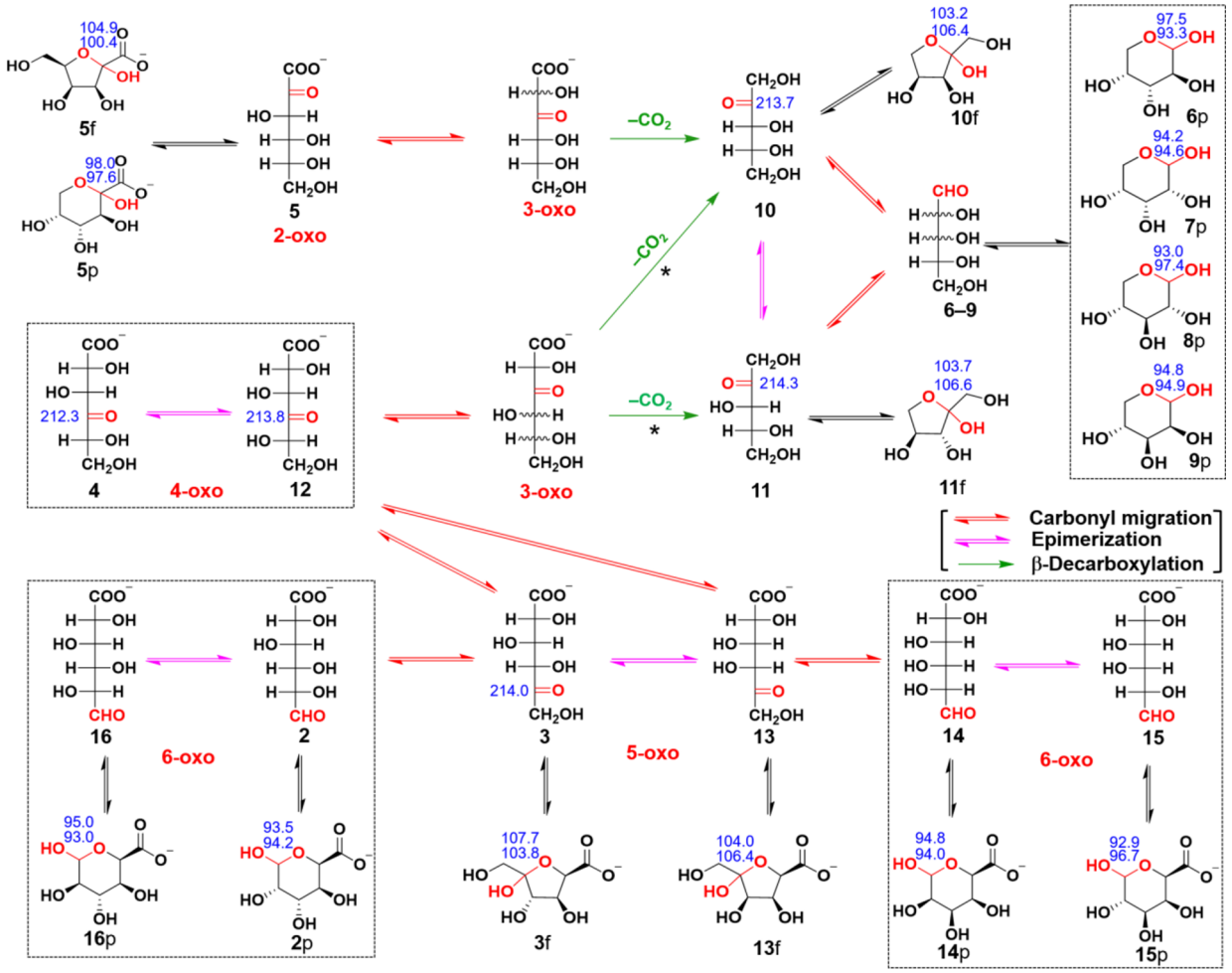

[a]The two asterisks (*) next to the green β-decarboxylation arrows indicate that these reactions can also produce the L-ketopentose enantiomers of **10** and **11** (not shown), thus also leading to the production of the L-aldopentoses of **6**−**9** (not shown). Note that all the structures containing chemical shifts (shown in blue) are detected in the ^{13}C NMR experiments carried out herein, and 3-oxo-uronate intermediates might also form a furanose ring, but are not shown here.

https://doi.org/10.1021/jacsau.3c00299
JACS Au 2023, 3, 2522−2535

form the most stable pyranose rings and require the most carbonyl migrations, followed by 5-oxo-uronates, which form less stable furanose rings, and fastest for the 4-oxo-uronates, which can only exist in their linear forms and require only one carbonyl migration. In comparison to 6-oxo-uronates, 2-oxo-uronates also form stable pyranose rings, however, only one carbonyl migration is required for the 2-oxo-uronates to yield 3-oxo-uronates. Moreover, enolization requires the carbonyl (unhydrated) form of the aldehyde or ketone to occur; the more electron-rich ketone carbons ought to be more resistant to hydration, undergoing enolization and therefore carbonyl migration at faster rates in comparison to aldehydes. Therefore, the rates of pentose production are much faster in 2-oxo-uronates than in 6-oxo-uronates. The ratio of pentoses formed is likely largely a function of their relative thermodynamic stabilities, especially at higher temperatures.

The formation of enediol(ate) intermediates is base-catalyzed and generally faster at higher temperatures.[72] Thus, higher temperatures and more alkaline pH should increase the observed rates of carbonyl migration, as well as increase the fraction of linear uronates at equilibrium with respect to the cyclic hemiacetals.[73] The 2-oxo-uronate **5** at pH 9 reacted at room temperature yielded a lower amount of total pentoses (∼10.5% after 56 days) compared to the reaction of **5** at pH 8 and 50 °C (∼30.6% after 24 days). There are, however, some mechanistic details with respect to temperature and pH dependencies of the carbonyl migration reactions which are still difficult to explain when comparing the 5-oxo-uronate **3** and the 6-oxo-uronates **15** and **17**. The 5-oxo-uronate **3** was reacted at pH 7, 8, and 9 at room temperature and 50 °C (Figures S24−S36). At room temperature, the rate of migration from the C5 to C3 position in slightly basic media (pH 8 and 9, Figures S24−S28) is significantly faster than at neutral pH (Figures S29 and S30). At 50 °C, however, the rate of carbonyl migration at pH 7, 8, and 9 are all similar (Figures S31−S36). In contrast, when the 6-oxo-uronates **15** (Figures S38−S44) and **17** (Figures S47−S53) were reacted at 50 °C, increasing the pH from 7 to 9 significantly accelerated the rate of carbonyl migration, and higher yields of the pentoses were obtained (Table 2). While it can be concluded that higher temperature increases the rate of carbonyl migration for all the uronates studied herein, why the effect of pH seems to change depending on the nature of the starting uronates and temperature of the reaction is not easily explicable. More detailed kinetic experiments are needed to elucidate these peculiarities.

Prebiotic Accumulation of Aldonates

Given the general instability of aldoses and ketoses in the context of early Earth aqueous geochemistry, if simple aldoses were important for the origins of life, for example, in the prebiotic synthesis of RNA, there must be specific mechanisms that mediate the electrophilicity of the carbonyl carbon for specific sugars to accumulate. In other words, one must invoke the use of "prebiotic protecting mechanisms" that act to inhibit the inherent reactivity of the electrophilic aldehyde or ketone to prevent their oligomerization into intractable tarlike materials that tend to take place over relatively short time scales, especially at extreme pH values and high temperatures. Instead of aldoses or ketoses, however, another possibility is the accumulation of aldonates,[29] which could have occurred as a consequence of the greater stability of their carboxylate anions, a functional group inherently resistant to nucleophilic addition/substitution under slightly acidic, neutral, or basic aqueous conditions. In fact, C3−C6 aldonates have been found in the Murchison meteorite.[31]

Aldonates are also natural end products of one of the most well-studied reactions for prebiotic sugar synthesis to date, namely, the Kiliani−Fischer homologation (Scheme 2a), which can be carried out under prebiotically plausible conditions[74−77] using hydrated electrons[74] as the reducing agent. The first step of the homologation cycle involves nucleophilic addition of HCN to the aldose/aldehyde carbonyl, affording a cyanohydrin intermediate. C4 and larger cyanohydrins have been shown to spontaneously undergo 5- or 6-membered-ring cyclization reactions by nucleophilic addition of a hydroxyl to the nitrile, yielding after elimination of NH_3 by hydrolysis, aldonic lactones.[78] These lactones can then undergo further hydrolysis to linear aldonates. Aldonate production from cyanohydrins takes place on a timescale of hours to days depending on temperature and pH, a fact which suggests that aldonate and sugar synthesis can occur in the same mixture given a suitable range of pH, temperature, and hydrated electron production.[78] Recently, Ritson and Sutherland reported the synthesis of tetroses and pentoses via prebiotic Kiliani−Fischer homologation starting from HCN.[45]

Unless the rate of reduction by hydrated electrons is quick enough to reduce the carboxylates of aldonates back to their aldehydes—which is unlikely at neutral and basic pH as a consequence of charge−charge repulsion[79]—prebiotic environments that facilitate the Kiliani−Fischer mechanism may also, over longer time scales, tend to accumulate the more stable aldonates rather than aldoses or ketoses. To test this hypothesis, when gluconate **1** at pH 4 (close to its pK_a) was subjected to gamma radiolysis, which generates a combination of hydrated electrons and hydroxyl radicals directly from water, hexoses were not detected, although the uronates **2**p, **4**, **3**f, and **5**f were formed, presumably through oxidation mediated by •OH (Figure S54). Hence, given an equal opportunity to undergo either reduction or oxidation, **1** preferentially undergoes oxidation to the mixture of uronates rather than reduction to glucose, even when a significant fraction of the conjugate acid of **1** is present. The Fenton reaction employed herein is also suspected to oxidize the aldonate **1** to uronates by in situ generation of hydroxyl radicals.

Whether or not a Fenton-type reaction mechanism could have occurred prebiotically has been debated.[80] While there is general consensus for the presence Fe(II) in early aqueous systems, the geochemical production of H_2O_2 during the Hadean may have been problematic, although there are recent suggestions that turbulent subaqueous environments can provide sufficient Archean H_2O_2.[46] The production of H_2O_2 has also been observed from silicate mineral weathering.[48]

The formose reaction is also known to generate short aldonates by Cannizzaro disproportionation of two aldoses/aldehydes into a (sugar) alcohol and a carboxylate (aldonate);[81,82] however, we were unable to find reports in the literature of Cannizzaro disproportionation occurring with larger aldoses (e.g., C6) to yield C6-aldonates. Nevertheless, the oxidation of hexoses that can be generated from the formose reaction does yield C6-aldonates (Figure S10).

One important caveat to note is the need of (semi)-periodically fluctuating pH from acidic to basic conditions. The Fenton oxidation occurs most efficiently under acidic conditions (pH 3−7), while the production of aldonates through the mechanisms discussed above along with the

https://doi.org/10.1021/jacsau.3c00299
JACS Au 2023, 3, 2522−2535

carbonyl migration network studied herein works best under slightly basic to highly basic conditions. Hydrothermal fields can give rise to clusters of subaerial hot spring pools in close proximity, each with unique pH, temperature, and dissolved ionic compositions.[83] Moreover, these pools are known to regularly mix with each other, and such hot spring environments may have provided the fluctuating pH conditions needed for this chemistry.

Comparison to the Pentose Phosphate Pathway

Core metabolism, in particular gluconeogenesis, glycolysis, and the PPP all rely on (enzymatic) carbonyl migration,[84,85] while the PPP also employs β-decarboxylation. It is not unreasonable to suppose that carbonyl migration and β-decarboxylation may have been heavily relied upon chemical transformations in protometabolic carbohydrate pathways prior to the advent of specialized enzymes or other catalytic polymers. A "glyoxylate scenario" employing glyoxylate and dihydroxyfumarate for the formation of sugars via β-decarboxylation and carbonyl migration has been proposed by Eschenmoser[86] and demonstrated by Sagi et al.[61] β-Decarboxylation is effectively irreversible and could provide a thermodynamic driving force that can direct reversible carbonyl migrations toward a single set of products, even in the absence of highly evolved, regiospecific enzymatic catalysis.

The pentose phosphate pathway employs regiospecific enzymatic oxidation of 6-phosphogluconate at its C3 position to enable β-decarboxylation in the next step that yields ribulose 5-phosphate. In the first oxidative phase, glucose 6-phosphate is oxidized enzymatically by $NADP^+$ to furnish 6-phosphogluconolactone (Scheme 2b), which hydrolyzes to 6-phophogluconate (the phosphorylated derivative of **1**). 6-Phosphogluconate is then thought[69,87] to be regioselectively oxidized at C3, generating a 6-phospho-3-oxo-uronate intermediate, that subsequently undergoes β-decarboxylation resulting in an enediol that isomerizes to ribulose 5-phosphate. The next steps in the PPP then involve enzymatic epimerization of ribulose 5-phosphate to xylulose 5-phosphate (not shown in the scheme), as well as carbonyl migration to generate ribose 5-phosphate. Ribose 5-phosphate is then shunted into the purine and pyrimidine biosynthesis and salvage pathways.[84]

The chemical pathways reported here resemble the first steps of the extant pentose phosphate pathway (Scheme 2). In the pathway demonstrated here, gluconate is nonselectively oxidized to all uronate regioisomers except the 3-oxo one, and this oxidation using the Fenton reaction can occur at both acidic and neutral pH, although Ruff degradation becomes dominant from pH 5 to 7. Some nonenzymatic pentose phosphate pathways have been reported by using Fe(II) or cysteine as a catalyst[2,3] to convert glucose-6-phosphate to ribose-5-phosphate proposed via gluconate-6-phosphate as an intermediate under acidic conditions, although the potential mechanism is still unknown since no gluconate-6-phosphate was detected in this system. The conversion of gluconate, however, directly to aldo- or ketopentoses by Fe(II) (without H_2O_2) was not observed in our study here. Furthermore, the oxidation of glucose to gluconate was also observed when glucose was subjected to Fenton reaction conditions (Figure S10). These results suggest that the above Fe(II) catalyzed conversion to ribose 5-phosphate does not proceed either through oxidation of glucose-6-phosphate to gluconate 6-phosphate or Ruff degradation followed by isomerization of arabinose-5-phosphate. It is possible that the organophosphate functionality has some effect on the mechanism not observed in our study.

The chemical pathways reported herein further suggest that oxidation of 6-phosphogluconate need not have always been regioselective in order to afford pentose phosphates in hypothetical early evolutionary forerunners to the PPP. No matter where oxidation takes place in the phosphoaldonate backbone, carbonyl migration has the potential to form the 3-oxo-intermediate that undergoes β-decarboxylation yielding pentose phosphates. It is tantalizing to speculate that the origins of the first few steps of the PPP may trace their roots back to protometabolism, when geochemically synthesized stockpiles of C6-aldonates served as "nutrients" that ancient protocellular metabolic networks could have exploited for pentose phosphate production using rudimentary catalysis, and that stereoselective pentose production evolved at a later stage. Note that Fenton oxidation of alanine did not take place when excess gluconate was present in the reaction mixture (Figures S55 and S56), an observation which suggests that as long as aldonates are abundant, the oxidization of other organic compounds, such as nucleotides and amino acids, might be minimized. The results demonstrated herein suggest a potential pathway for how the production of sugars via the Kiliani–Fischer mechanism could have transitioned into chemistry more reminiscent of extant biochemical mechanisms. Coincidentally, some bacteria in the absence of sugars like glucose are known to be capable of surviving on gluconate, a substrate which gets diverted to either the PPP or the Entner–Doudoroff pathways.[88−90] However, it is also important to keep in mind that such speculative extrapolations need to be tempered with caution as there may have been early pathways that may have been lost forever. Such observations may "not necessarily indicate an evolutionary continuity between prebiotic chemistry and biochemical pathways".[7]

CONCLUSIONS

In the presence of ferrous iron and hydrogen peroxide, C6-aldonates, including gluconate, undergo nonregioselective oxidation to yield a mixture of 6-oxo-, 5-oxo-, 4-oxo-, and 2-oxo-uronate regioisomers. These uronate isomers undergo carbonyl migration under weakly basic or neutral conditions to yield 3-oxo-uronates that undergo facile β-decarboxylation to generate all four pentoses. The major pathway for carbonyl migration likely involves the base-catalyzed formation of enediol(ate) intermediates, a proposed mechanism supported by mass spectrometry. The rate of carbonyl migration depends on (i) the fraction of linear uronates in solution with respect to their cyclic hemiacetals, since only the linear isomers are capable of forming enediol(ate)s and (ii) the number of carbonyl migrations needed to yield the 3-oxo-uronate intermediates. Consequently, the rates of pentose production display the following order from the slowest to the fastest (see Table 2): 6-oxo-uronates, which prefer the more stable pyranose rings and require the most number (three) of carbonyl migrations to form the 3-oxo-uronates; 5-oxo-uronates, which exist as less stable furanose rings and require two carbonyl migrations; 2-oxo-uronates, which still form stable cyclic hemiacetals, but are structurally only capable of carbonyl migration directly to the 3-oxo-uronate; and fastest for the 4-oxo-uronates, which exist as linear ketones, and require in principle only one carbonyl migration. This chemistry that converts aldonates to uronates to pentoses may have been relevant to prebiotic chemistry of sugar

https://doi.org/10.1021/jacsau.3c00299
JACS Au 2023, 3, 2522−2535

formation and perhaps served as a forerunner for some of the chemistries observed in the extant PPP biochemical pathways. We plan to explore potential methods to increase the yield and selectivity of pentose generation, for example, through the use of simple peptides.

METHODS

Oxidation of Gluconate 1

A 1 mL solution containing 500 mM sodium gluconate **1** (109 mg, 0.5 mmol) and 25 mM $Fe(OAc)_2$ (4.3 mg, 0.025 mmol) was prepared in a 2 mL Eppendorf tube, and the pH was adjusted to 3. The solution was cooled in an ice bath, and 43 μL of hydrogen peroxide (35% in water) was added. The mixture was warmed to room temperature. After 2 h, in order to stop the reaction and remove the free iron cation, about 500 mg of DOWEX 50Wx4 100−200 mesh (H^+) cation exchange resin was added to the reaction mixture. Then, the tube was vortexed for 2 min, and the resin was filtered. In order to improve the resolution of the resonances in the ^{13}C-NMR spectra and to avoid the formation of lactone, 400 μL of the filtered solution was mixed with 50 μL of 1 M P_i at pH 7.5, along with 50 μL of D_2O and 2 μL of DMSO. The pH was then adjusted to 7.5 as needed and measured by NMR at 25 °C (Figure S1).

Irradiation of Aqueous Gluconate Solutions

A 2 mL aqueous solution containing 500 mM sodium gluconate (218 mg, 1.0 mmol) was prepared at pH 4 using HCl and placed into a crimp-sealed vial. Then, the vial was exposed to γ-radiation for 24 h (total dose: ∼72 kGy at ∼3 kGy h^{-1}) at ∼25 °C. After exposure, 400 μL of solution was mixed with 50 μL of 1 M sodium phosphate buffer, along with 50 μL of D_2O and 2 μL of DMSO as a standard. In order to improve the resolution of the resonances in the ^{13}C NMR spectra, the pH was then adjusted to 7.5, and the NMR spectra were recorded at 25 °C (see Figure S54).

Carbonyl Migration of 2-Keto-D-gluconate 5

A 1 mL solution containing 500 mM 2-keto-D-gluconic acid hemicalcium salt (107 mg, 0.5 mmol) in 10% D_2O was prepared. To remove the Ca^{2+} cation, about 500 mg of DOWEX 50Wx4 100−200 mesh (H) cation exchange resin was added to the reaction mixture. The resin was filtered. Then, 500 mL of filtered solution was mixed with Na_3PO_4 (74 mg), and the pH was adjusted to 8. This solution was loaded into an NMR tube and heated at 50 °C (Figures S11−S13).

Thermodynamic Study of the Pentose Distribution

A 500 μL solution containing 250 mM each of ribose, arabinose, lyxose, xylose (18.8 mg, 0.125 mmol), 0.8 M P_i, and 2 μL and DMSO in 10% D_2O was prepared, and the pH was adjusted to 8. This solution was loaded into an NMR tube and heated at 50 °C (Figures S16−S18).

Carbonyl Migration of D-Xylo-4-hexulosonate 4

A 500 μL solution containing 500 mM D-*xylo*-4-hexulosonic acid **4** (48.5 mg, 0.25 mmol), 0.9 M P_i, and 2 μL of DMSO in 10% D_2O was prepared, and the pH was adjusted to 9. The mixture was transferred to an NMR tube and monitored by ^{13}C NMR spectroscopy over time at room temperature (Figures S19−S23).

Carbonyl Migration of 5-Keto-D-gluconate 3

A 500 μL solution containing 500 mM 5-keto-D-gluconic acid potassium salt (58 mg, 0.25 mmol), 0.9 M P_i, and 2 μL of DMSO in 10% D_2O was prepared, and the pH was adjusted to 9. The mixture was transferred to an NMR tube and monitored by ^{13}C NMR spectroscopy at room temperature (Figures S24−S26).

Carbonyl Migration of D-Galacturonate 15

A 500 μL solution containing 500 mM D-galacturonic acid monohydrate (53 mg, 0.25 mmol), 0.9 M P_i, and 2 μL of DMSO in 10% D_2O was prepared, and the pH was adjusted to 9. The mixture was transferred to an NMR tube and monitored by ^{13}C NMR spectroscopy at room temperature (Figure 5).

Carbonyl Migration of D-Glucuronate 17

A 500 μL solution containing 500 mM D-glucuronic acid sodium salt monohydrate (58.5 mg, 0.25 mmol), 0.9 M P_i, and 2 μL of DMSO in 10% D_2O was prepared, and the pH was adjusted to 9. The mixture was transferred to an NMR tube and monitored by ^{13}C NMR spectroscopy at room temperature (Figures S45 and S46).

ASSOCIATED CONTENT

Supporting Information

The Supporting Information is available free of charge at https://pubs.acs.org/doi/10.1021/jacsau.3c00299.

General methods, NMR spectroscopy, HPLC, and mass spectrometry (PDF)

AUTHOR INFORMATION

Corresponding Authors

Ruiqin Yi − *Earth-Life Science Institute, Tokyo Institute of Technology, Tokyo 152-8550, Japan;* orcid.org/0000-0003-2393-700X; Email: yiruiqin@elsi.jp

Ramanarayanan Krishnamurthy − *Department of Chemistry, The Scripps Research Institute, La Jolla, California 92037, United States;* orcid.org/0000-0001-5238-610X; Email: rkrishna@scripps.edu

Charles L. Liotta − *School of Chemistry and Biochemistry, Georgia Institute of Technology, Atlanta, Georgia 30332, United States;* orcid.org/0000-0002-7450-6640; Email: charles.liotta@carnegie.gatech.edu

Authors

Mike Mojica − *School of Chemistry and Biochemistry, Georgia Institute of Technology, Atlanta, Georgia 30332, United States*

Albert C. Fahrenbach − *School of Chemistry, Australian Centre for Astrobiology and the UNSW RNA Institute, University of New South Wales, Sydney, NSW 2052, Australia;* orcid.org/0000-0002-8315-8836

H. James Cleaves, II − *Blue Marble Space Institute of Science, Seattle, Washington 98154, United States;* Present Address: Department of Chemistry, Howard University, 525 College Street, NW, Room 120, Washington, D.C. 20059, United States; orcid.org/0000-0003-4101-0654

Complete contact information is available at: https://pubs.acs.org/10.1021/jacsau.3c00299

Author Contributions

C.L.L. and R.K. conceived the project. R.Y. and C.L.L. designed the experiments, and R.Y. carried out experiments presented in the manuscript. R.Y., A.C.F., and H.J.C. analyzed the data. M.M. carried out preliminary experiments. All authors contributed to the writing of the manuscript.

Notes

The authors declare no competing financial interest.

ACKNOWLEDGMENTS

This work was supported by the NASA Exobiology Program NNH20ZA001N-EXO Grant 20-EXO-0006 and jointly by National Science Foundation and the NASA Astrobiology Program under the Center for Chemical Evolution grant no. CHE-1504217. This work was also supported by the

Astrobiology Center Program of National Institutes of Natural Sciences (NINS) (Grant Number AB031017), Japan Society for the Promotion of Science (JSPS) Grant-in-aid 21 K14029, and by the WPI-funded Earth-Life Science institute at the Tokyo Institute of Technology. A.C.F acknowledges support from the University of New South Wales Strategic Hires and Retention Pathways (SHARP) program and the Australian Research Council Discovery Project Grant DP210102133 and Future Fellowship (FT220100757).

REFERENCES

(1) Ruiz-Mirazo, K.; Briones, C.; De La Escosura, A. Prebiotic Systems Chemistry: New Perspectives for the Origins of Life. *Chem. Rev.* **2014**, *114*, 285−366.
(2) Keller, M. A.; Turchyn, A. V.; Ralser, M. Non-enzymatic Glycolysis and Pentose Phosphate Pathway-like Reactions in a Plausible A Rchean Ocean. *Mol. Syst. Biol.* **2014**, *10*, 725.
(3) Keller, M. A.; Zylstra, A.; Castro, C.; Turchyn, A. V.; Griffin, J. L.; Ralser, M. Conditional Iron and PH-Dependent Activity of a Non-Enzymatic Glycolysis and Pentose Phosphate Pathway. *Sci. Adv.* **2016**, *2*, No. e1501235.
(4) Goldford, J. E.; Segrè, D. Modern Views of Ancient Metabolic Networks. *Curr. Opin. Syst. Biol.* **2018**, *8*, 117−124.
(5) Krishnamurthy, R. Systems Chemistry in the Chemical Origins of Life: The 18th Camel Paradigm. *J. Syst. Chem* **2020**, *8*, 40−62.
(6) Arya, A.; Ray, J.; Sharma, S.; Simbron, R. C.; Lozano, A.; Smith, H. B.; Andersen, J. L.; Chen, H.; Meringer, M.; Cleaves, H. J. An Open Source Computational Workflow for the Discovery of Autocatalytic Networks in Abiotic Reactions. *Chem. Sci.* **2022**, *13*, 4838−4853.
(7) Lazcano, A.; Miller, S. L. On the Origin of Metabolic Pathways. *J. Mol. Evol.* **1999**, *49*, 424−431.
(8) Krishnamurthy, R. Life's Biological Chemistry: A Destiny or Destination Starting from Prebiotic Chemistry? *Chem. − Eur. J.* **2018**, *24*, 16708−16715.
(9) Muchowska, K. B.; Varma, S. J.; Moran, J. Nonenzymatic Metabolic Reactions and Life's Origins. *Chem. Rev.* **2020**, *120*, 7708−7744.
(10) Stubbs, R. T.; Yadav, M.; Krishnamurthy, R.; Springsteen, G. A Plausible Metal-Free Ancestral Analogue of the Krebs Cycle Composed Entirely of α-Ketoacids. *Nat. Chem.* **2020**, *12*, 1016−1022.
(11) Pulletikurti, S.; Yadav, M.; Springsteen, G.; Krishnamurthy, R. Prebiotic Synthesis of α-Amino Acids and Orotate from α-Ketoacids Potentiates Transition to Extant Metabolic Pathways. *Nat. Chem.* **2022**, *14*, 1142−1150.
(12) Yadav, M.; Pulletikurti, S.; Yerabolu, J. R.; Krishnamurthy, R. Cyanide as a Primordial Reductant Enables a Protometabolic Reductive Glyoxylate Pathway. *Nat. Chem.* **2022**, *14*, 170−178.
(13) Butlerow, A. Formation Synthétique d'une Substance Sucrée. *CR Acad. Sci.* **1861**, *53*, 145−147.
(14) Breslow, R. On the Mechanism of the Formose Reaction. *Tetrahedron Lett.* **1959**, *1*, 22−26.
(15) Shapiro, R. Prebiotic Ribose Synthesis: A Critical Analysis. *Orig. Life Evol. Biosph.* **1988**, *18*, 71−85.
(16) Cleaves, H. J. The Prebiotic Geochemistry of Formaldehyde. *Precambrian Res.* **2008**, *164*, 111−118.
(17) Appayee, C.; Breslow, R. Deuterium Studies Reveal a New Mechanism for the Formose Reaction Involving Hydride Shifts. *J. Am. Chem. Soc.* **2014**, *136*, 3720−3723.
(18) Ricardo, A.; Frye, F.; Carrigan, M. A.; Tipton, J. D.; Powell, D. H.; Benner, S. A. 2-Hydroxymethylboronate as a Reagent to Detect Carbohydrates: Application to the Analysis of the Formose Reaction. *J. Org. Chem.* **2006**, *71*, 9503−9505.
(19) Prieur, B. E. Étude de l'activité Prébiotique Potentielle de l'acide Borique. *Comptes Rendus l'Académie des Sci. IIC-Chemistry* **2001**, *4*, 667−670.
(20) Ricardo, A.; Carrigan, M. A.; Olcott, A. N.; Benner, S. A. Borate Minerals Stabilize Ribose. *Science* **2004**, *303*, 196.
(21) Kim, H.-J.; Ricardo, A.; Illangkoon, H. I.; Kim, M. J.; Carrigan, M. A.; Frye, F.; Benner, S. A. Synthesis of Carbohydrates in Mineral-Guided Prebiotic Cycles. *J. Am. Chem. Soc.* **2011**, *133*, 9457−9468.
(22) Mizuno, T.; Weiss, A. H. Synthesis and Utilization of Formose Sugars. In *Advances in carbohydrate chemistry and biochemistry*; Elsevier, 1974; Vol. *29*; pp 173−227.
(23) Zubay, G.; Mui, T. Prebiotic Synthesis of Nucleotides. *Origins Life Evol. Biospheres* **2001**, *31*, 87−102.
(24) Cleaves, H. J. Formose Reaction. In *Encyclopedia of Astrobiology*; Gargaud, M.; Amils, R.; Quintanilla, J. C.; Cleaves, H. J.; Irvine, W. M.; Pinti, D. L.; Viso, M., Eds.; Springer Berlin Heidelberg: Berlin, Heidelberg, 2011; pp 600−605.
(25) Islam, S.; Powner, M. W. Prebiotic Systems Chemistry: Complexity Overcoming Clutter. *Chem* **2017**, *2*, 470−501.
(26) Benner, S. A.; Kim, H.-J.; Biondi, E. Prebiotic Chemistry That Could Not Not Have Happened. *Life* **2019**, *9*, 84.
(27) Shapiro, R. The Prebiotic Role of Adenine: A Critical Analysis. *Origins Life Evol. Biospheres* **1995**, *25*, 83−98.
(28) Shapiro, R. Prebiotic Cytosine Synthesis: A Critical Analysis and Implications for the Origin of Life. *Proc. Natl. Acad. Sci. U. S. A.* **1999**, *96*, 4396−4401.
(29) Larralde, R.; Robertson, M. P.; Miller, S. L. Rates of Decomposition of Ribose and Other Sugars: Implications for Chemical Evolution. *Proc. Natl. Acad. Sci. U. S. A.* **1995**, *92*, 8158−8160.
(30) Varma, R.; French, D. Mechanism of the Cyanohydrin (Kiliani-Fischer) Synthesis. *Carbohydr. Res.* **1972**, *25*, 71−79.
(31) Cooper, G.; Kimmich, N.; Belisle, W.; Sarinana, J.; Brabham, K.; Garrel, L. Carbonaceous Meteorites as a Source of Sugar-Related Organic Compounds for the Early Earth. *Nature* **2001**, *414*, 879−883.
(32) Furukawa, Y.; Chikaraishi, Y.; Ohkouchi, N.; Ogawa, N. O.; Glavin, D. P.; Dworkin, J. P.; Abe, C.; Nakamura, T. Extraterrestrial Ribose and Other Sugars in Primitive Meteorites. *Proc. Natl. Acad. Sci. U. S. A.* **2019**, *116*, 24440−24445.
(33) Fenton, H. J. H.; Jones, H. O. VII.—The Oxidation of Organic Acids in Presence of Ferrous Iron. Part I. *J. Chem. Soc., Trans.* **1900**, *77*, 69−76.
(34) Krishnamurthy, R.; Liotta, C. L. The Potential of Glyoxylate as a Prebiotic Source Molecule and a Reactant in Protometabolic Pathways—The Glyoxylose Reaction. *Chem* **2023**, *9*, 784−797.
(35) Sowden, J. C.; Schaffer, R. The Isomerization of D-Glucose by Alkali in D2O at 25°. *J. Am. Chem. Soc.* **1952**, *74*, 505−507.
(36) Schaffer, R. The Isomerization of D-Manno-3-Heptulose by Alkali. *J. Org. Chem.* **1964**, *29*, 1473−1475.
(37) Yaylayan, V. A.; Ismail, A. A. Investigation of the Enolization and Carbonyl Group Migration in Reducing Sugars by FTIR Spectroscopy. *Carbohydr. Res.* **1995**, *276*, 253−265.
(38) Angyal, S. J. The Lobry de Bruyn-Alberda van Ekenstein Transformation and Related Reactions. In *Glycoscience*; Springer, 2001; pp 1−14.
(39) Angyal, S. J. A Short Note on the Epimerization of Aldoses. *Carbohydr. Res.* **1997**, *300*, 279−281.
(40) Tanase, T.; Shimizu, F.; Kuse, M.; Yano, S.; Hidai, M.; Yoshikawa, S. Novel C-2 Epimerization of Aldoses Promoted by Nickel (II) Diamine Complexes, Involving a Stereospecific Pinacol-Type 1, 2-Carbon Shift. *Inorg. Chem.* **1988**, *27*, 4085−4094.
(41) Yi, R.; Kern, R.; Pollet, P.; Lin, H.; Krishnamurthy, R.; Liotta, C. L. Erythrose and Threose: Carbonyl Migrations, Epimerizations, Aldol, and Oxidative Fragmentation Reactions Under Plausible Prebiotic Conditions. *Chem. − Eur. J.* **2023**, *29*, No. e202202816.
(42) Reihl, O.; Rothenbacher, T. M.; Lederer, M. O.; Schwack, W. Carbohydrate Carbonyl Mobility−−the Key Process in the Formation of α-Dicarbonyl Intermediates. *Carbohydr. Res.* **2004**, *339*, 1609−1618.
(43) Horvat, Š.; Roščić, M.; Lemieux, C.; Nguyen, T. M.; Schiller, P. W. Formation Pathways and Opioid Activity Data for 3-Hydroxypyridinium Compounds Derived from Glucuronic Acid and Opioid Peptides by Maillard Processes. *Chem. Biol. Drug Des.* **2007**, *70*, 30−39.

https://doi.org/10.1021/jacsau.3c00299
JACS Au 2023, 3, 2522−2535

(44) Horvat, Š.; Roščić, M. Glycosylation of Lysine-Containing Pentapeptides by Glucuronic Acid: New Insights into the Maillard Reaction. *Carbohydr. Res.* **2010**, *345*, 377−384.
(45) Ritson, D. J.; Sutherland, J. D. Thiophosphate Photochemistry Enables Prebiotic Access to Sugars and Terpenoid Precursors. *Nat. Chem.* **2023**, 1−8.
(46) He, H.; Wu, X.; Xian, H.; Zhu, J.; Yang, Y.; Lv, Y.; Li, Y.; Konhauser, K. O. An Abiotic Source of Archean Hydrogen Peroxide and Oxygen That Pre-Dates Oxygenic Photosynthesis. *Nat. Commun.* **2021**, *12*, 6611.
(47) Omran, A.; Abbatiello, J.; Feng, T.; Pasek, M. A. Oxidative Phosphorus Chemistry Perturbed by Minerals. *Life* **2022**, *12*, 198.
(48) He, H.; Wu, X.; Zhu, J.; Lin, M.; Lv, Y.; Xian, H.; Yang, Y.; Lin, X.; Li, S.; Li, Y.; Teng, H. H.; Thiemens, M. H. A Mineral-Based Origin of Earth's Initial Hydrogen Peroxide and Molecular Oxygen. *Proc. Natl. Acad. Sci. U. S. A.* **2023**, *120*, No. e2221984120.
(49) Larsen, B.; Smisrod, O. The Effect of PH and Buffer Ions on the Degradation of Carbohydrates by Fenton's Reagent. *Acta Chem. Scand.* **1967**, *21*, 552−564.
(50) Barb, W. G.; Baxendale, J. H.; George, P.; Hargrave, K. R. Reactions of Ferrous and Ferric Ions with Hydrogen Peroxide. Part I.—The Ferrous Ion Reaction. *Trans. Faraday Soc.* **1951**, *47*, 462−500.
(51) Stapley, J. A.; BeMiller, J. N. The Ruff Degradation: A Review of Previously Proposed Mechanisms with Evidence That the Reaction Proceeds by a Hofer-Moest-Type Reaction. *Carbohydr. Res.* **2007**, *342*, 407−418.
(52) Zazo, J. A.; Pliego, G.; Blasco, S.; Casas, J. A.; Rodriguez, J. J. Intensification of the Fenton Process by Increasing the Temperature. *Ind. Eng. Chem. Res.* **2011**, *50*, 866−870.
(53) Ashwell, G.; Kanfer, J.; Smiley, J. D.; Burns, J. J. Metabolism of Ascorbic Acid and Related Uronic Acids, Aldonic Acids, and Pentoses. *Ann. N. Y. Acad. Sci.* **1961**, *92*, 105−114.
(54) Smiley, J. D.; Ashwell, G. Purification and Properties of β-l-Hydroxy Acid Dehydrogenase. *J. Biol. Chem.* **1961**, *236*, 357−364.
(55) Hall, A. N.; Kulka, D.; Walker, T. K. Formation of Arabinose, Ribulose and Tartronic Acid from 2-Keto-d-Gluconic Acid. *Biochem. J.* **1955**, *60*, 271.
(56) Toner, J. D.; Catling, D. C. A Carbonate-Rich Lake Solution to the Phosphate Problem of the Origin of Life. *Proc. Natl. Acad. Sci. U. S. A.* **2020**, *117*, 883−888.
(57) Getenet, M.; García-Ruiz, J. M.; Otálora, F.; Emmerling, F.; Al-Sabbagh, D.; Verdugo-Escamilla, C. A Comprehensive Methodology for Monitoring Evaporitic Mineral Precipitation and Hydrochemical Evolution of Saline Lakes: The Case of Lake Magadi Soda Brine (East African Rift Valley, Kenya). *Cryst. Growth Des.* **2022**, *22*, 2307−2317.
(58) Delidovich, I.; Gyngazova, M. S.; Sánchez-Bastardo, N.; Wohland, J. P.; Hoppe, C.; Drabo, P. Production of Keto-Pentoses: Via Isomerization of Aldo-Pentoses Catalyzed by Phosphates and Recovery of Products by Anionic Extraction. *Green Chem.* **2018**, *20*, 724−734.
(59) Crawford, T. C.; Andrews, G. C.; Faubl, H.; Chmurny, G. N. The Structure of Biologically Important Carbohydrates. A Carbon-13 Nuclear Magnetic Resonance Study of Tautomeric Equilibriums in Several Hexulosonic Acids and Related Compounds. *J. Am. Chem. Soc.* **1980**, *102*, 2220−2225.
(60) Dorman, D. E.; Roberts, J. D. Nuclear Magnetic Resonance Spectroscopy. Carbon-13 Spectra of Some Pentose and Hexose Aldopyranoses. *J. Am. Chem. Soc.* **1970**, *92*, 1355−1361.
(61) Sagi, V. N.; Punna, V.; Hu, F.; Meher, G.; Krishnamurthy, R. Exploratory Experiments on the Chemistry of the "Glyoxylate Scenario": Formation of Ketosugars from Dihydroxyfumarate. *J. Am. Chem. Soc.* **2012**, *134*, 3577−3589.
(62) Lopalco, A.; Dalwadi, G.; Niu, S.; Schowen, R. L.; Douglas, J.; Stella, V. J. Mechanism of Decarboxylation of Pyruvic Acid in the Presence of Hydrogen Peroxide. *J. Pharm. Sci.* **2016**, *105*, 705−713.
(63) Onoda, H.; Shoji, O.; Suzuki, K.; Sugimoto, H.; Shiro, Y.; Watanabe, Y. α-Oxidative Decarboxylation of Fatty Acids Catalysed by Cytochrome P450 Peroxygenases Yielding Shorter-Alkyl-Chain Fatty Acids. *Catal. Sci. Technol.* **2018**, *8*, 434−442.
(64) Gangadurai, C.; Illa, G. T.; Reddy, D. S. FeCl 3-Catalyzed Oxidative Decarboxylation of Aryl/Heteroaryl Acetic Acids: Preparation of Selected API Impurities. *Org. Biomol. Chem.* **2020**, *18*, 8459−8466.
(65) MadalenaáCaldeira, M.; Bekkum, H. The Structure of D-Xylo-5-Hexulosonic Acid and Its Gadolinium (III) Complexes in Aqueous Medium as Studied by Nuclear Magnetic Resonance. *J. Chem. Soc., Dalton Trans.* **1990**, *9*, 2707−2711.
(66) Luisa, M.; Ramos, D.; Madalena, M.; Caldeira, M.; Gil, V. M. S. NMR Study of Uronic Acids and Their Complexation with Molybdenum (VI) and Tungsten (VI) Oxoions. *Carbohydr. Res.* **1996**, *286*, 1−15.
(67) Quemener, B.; Lahaye, M.; Bobin-Dubigeon, C. Sugar Determination in Ulvans by a Chemical-Enzymatic Method Coupled to High Performance Anion Exchange Chromatography. *J. Appl. Phycol.* **1997**, *9*, 179−188.
(68) Vuorinen, T.; Serianni, A. S. Synthesis of D-Erythro-2-Pentulose and D-Threo-2-Pentulose and Analysis of the 13C-and 1H-Nmr Spectra of the 1-13C-and 2-13C-Substituted Sugars. *Carbohydr. Res.* **1991**, *209*, 13−31.
(69) Topham, C. M.; Dalziel, K. The Chemical Mechanism of Sheep Liver 6-Phosphogluconate Dehydrogenase. A Schiff-Base Intermediate Is Not Involved. *Biochem. J.* **1986**, *234*, 671−677.
(70) Angyal, S. J. The Composition and Conformation of Sugars in Solution. *Angew. Chem., Int. Ed. Engl.* **1969**, *8*, 157−166.
(71) Tewari, Y. B.; Goldberg, R. N. An Investigation of the Equilibria between Aqueous Ribose, Ribulose, and Arabinose. *Biophys. Chem.* **1985**, *22*, 197−204.
(72) El Khadem, H. S.; Ennifar, S.; Isbell, H. S. Evidence of Stable Hydrogen-Bonded Ions during Isomerization of Hexoses in Alkali. *Carbohydr. Res.* **1989**, *185*, 51−59.
(73) Yaylayan, V. A.; Ismail, A. A. Determination of the Effect of Temperature on the Concentration of Keto Form of D-Fructose by FT-IR Spectroscopy. *J. Carbohydr. Chem.* **1992**, *11*, 149−158.
(74) Ritson, D.; Sutherland, J. D. Prebiotic Synthesis of Simple Sugars by Photoredox Systems Chemistry. *Nat. Chem.* **2012**, *4*, 895−899.
(75) Yi, R.; Hongo, Y.; Yoda, I.; Adam, Z. R.; Fahrenbach, A. C. Radiolytic Synthesis of Cyanogen Chloride Cyanamide and Simple Sugar Precursors. *ChemistrySelect* **2018**, *3*, 10169−10174.
(76) Yi, R.; Tran, Q. P.; Ali, S.; Yoda, I.; Adam, Z. R.; Cleaves, H. J.; Fahrenbach, A. C. A Continuous Reaction Network That Produces RNA Precursors. *Proc. Natl. Acad. Sci. U. S. A.* **2020**, *117*, 13267−13274.
(77) Liu, Z.; Wu, L.-F.; Bond, A. D.; Sutherland, J. D. Photoredox Chemistry in the Synthesis of 2-Aminoazoles Implicated in Prebiotic Nucleic Acid Synthesis. *Chem. Commun.* **2020**, *56*, 13563−13566.
(78) Serianni, A. S.; Nunez, H. A.; Barker, R. Cyanohydrin Synthesis: Studies with Carbon-13-Labeled Cyanide. *J. Org. Chem.* **1980**, *45*, 3329−3341.
(79) Buxton, G. V.; Greenstock, C. L.; Helman, W. P.; Ross, A. B. Critical Review of Rate Constants for Reactions of Hydrated Electrons, Hydrogen Atoms and Hydroxyl Radicals (·OH/·O−) in Aqueous Solution. *J. Phys. Chem. Ref. Data* **1988**, *17*, 513−886.
(80) Ritson, D. J.; Mojzsis, S. J.; Sutherland, J. Supply of Phosphate to Early Earth by Photogeochemistry after Meteoritic Weathering. *Nat. Geosci.* **2020**, *13*, 344−348.
(81) Weiss, A. H.; LaPierre, R. B.; Shapira, J. Homogeneously Catalyzed Formaldehyde Condensation to Carbohydrates. *J. Catal.* **1970**, *16*, 332−347.
(82) Omran, A.; Menor-Salvan, C.; Springsteen, G.; Pasek, M. The Messy Alkaline Formose Reaction and Its Link to Metabolism. *Life* **2020**, *10*, 125.
(83) Damer, B.; Deamer, D. The Hot Spring Hypothesis for an Origin of Life. *Astrobiology* **2020**, *20*, 429−452.

https://doi.org/10.1021/jacsau.3c00299
JACS Au 2023, 3, 2522−2535

(84) Smith, E.; Morowitz, H. J. *The Origin and Nature of Life on Earth: The Emergence of the Fourth Geosphere*; Cambridge University Press, 2016; pp 35−72.
(85) Ter-Ovanessian, L. M. P.; Rigaud, B.; Mezzetti, A.; Lambert, J.-F.; Maurel, M.-C. Carbamoyl Phosphate and Its Substitutes for the Uracil Synthesis in Origins of Life Scenarios. *Sci. Rep.* **2021**, *11*, 19356.
(86) Eschenmoser, A. The Search for the Chemistry of Life's Origin. *Tetrahedron* **2007**, *63*, 12821−12844.
(87) Hwang, C.-C.; Berdis, A. J.; Karsten, W. E.; Cleland, W. W.; Cook, P. F. Oxidative Decarboxylation of 6-Phosphogluconate by 6-Phosphogluconate Dehydrogenase Proceeds by a Stepwise Mechanism with NADP and APADP as Oxidants. *Biochemistry* **1998**, *37*, 12596−12602.
(88) Horecker, B. L.; Mehler, A. H. Carbohydrate Metabolism. *Annu. Rev. Biochem.* **1955**, *24*, 207−274.
(89) Sokatch, J. T.; Gunsalus, I. C. Aldonic Acid Metabolism. I. Pathway of Carbon in an Inducible Gluconate Fermentation by Streptococcus Faecalis. *J. Bacteriol.* **1957**, *73*, 452−460.
(90) Ma, Y.; Li, B.; Zhang, X.; Wang, C.; Chen, W. Production of Gluconic Acid and Its Derivatives by Microbial Fermentation: Process Improvement Based on Integrated Routes. *Front. Bioeng. Biotechnol.* **2022**, 10.
(91) Regna, P. P.; Caldwell, B. P. Kinetics of Transformation of 2-Ketopolyhydroxy Acids. *J. Am. Chem. Soc.* **1944**, *66*, 246−250.

https://doi.org/10.1021/jacsau.3c00299
JACS Au 2023, 3, 2522−2535